Downward Surface Diffuse Solar Irradiances in Clear Atmospheres: Comparison Between Model and Observations

Q. Fu, G. Lesins, W. B. Sun, and J. Higgins
Dalhousie University
Halifax, Nova Scotia, Canada

Abstract

A data set collected at the Atmospheric Radiation Measurement (ARM) Southern Great Plains (SGP) central facility is analyzed to examine the downward surface diffuse solar irradiances under clear-sky conditions in the summer of 1996. A comparison between model and observations reveals that the model overestimates diffuse irradiance by ~22 W m^{-2} out of an average of ~98 W m^{-2}. In the model simulation, the aerosol single-scattering albedo and asymmetry factor is based on the d'Almeida rural aerosol. In this study, we attempt to find possible explanations for this discrepancy by investigating the potential measurement errors and uncertainties related to the radiative transfer input data. A hypothesis regarding the effects of aerosol size distributions is examined in an attempt to bring the model results into agreement with observations.

Introduction

The transfer of solar and terrestrial radiation in the atmosphere represents the prime physical process that drives the atmospheric circulation. The accurate modeling of this process is essential to the general circulation model (GCM) predictions of climate change, which require closure experiments to evaluate radiation simulations using atmospheric radiation measurements (Stokes and Schwartz 1994).

Several recent studies indicate that the clear-sky downward solar surface irradiances from models exceed observations (Charlock and Alberta 1996; Kato et al. 1997; Kinne et al. 1998). These studies suggested that the discrepancy is largely associated with the diffuse field irradiances. However, physical mechanisms responsible for this discrepancy remain uncertain.

In this study, we examine the downward surface diffuse solar irradiances under clear-sky conditions using a data set obtained from the ARM SGP central facility in Oklahoma in the summer of 1996. A comparison between model calculations and observations is performed to identify the magnitude of the disagreement. We attempt to find possible explanations for this discrepancy by investigating the potential measurement errors and uncertainties related to model simulations. A hypothesis regarding the effects of the aerosol size distribution is examined in an attempt to bring the model results into agreement with observations.

Comparison of Model Simulations to Observations

The solar radiation measurements were taken from the Baseline Solar Radiation Network (BSRN) system, which provides 1-minute averages of the downward solar diffuse, normal direct, and total irradiances at the surface. The observational site is located at the ARM SGP central facility. Measurements taken between 1 July and 11 September of 1996 are analyzed and we focus on the downward diffuse irradiances from the BSRN shaded pyranometer.

In this study, only clear-sky periods no shorter than 30 minutes are considered. Using the total optical depths derived from narrowband direct irradiances measured by a Multi-Filter Rotating Shadowband Radiometer (MFRSR), 159 30-minute segments for the summer of 1996 are classified as cases without clouds blocking the direct sunlight (Fu et al. 1997). To further identify the cases for diffuse irradiances under clear-sky conditions, the time series of the diffuse irradiance, with 1-minute resolution from BSRN, is plotted for each 30-minute segment and a linear fit is made to the data. If any point deviates by more than 2.5 W m^{-2} from this fitting, we consider the data contaminated by cloud and the segment is rejected. We also exclude cases where the solar zenith angle is larger than 72.5° because the effect of spherical atmospheres can be significant. Using the above procedures, we identify 119 cases for the summer 1996 period as clear-sky radiation measurements.

To compare radiative fluxes between the model and measurements, data serving as model input such as aerosol single-scattering properties, atmospheric pressure, temperature, water vapor, and ozone profiles, are needed. Pressure, temperature, and water vapor profiles were derived from radiosondes at the ARM SGP central facility (Fu et al. 1997). The standard mid-latitude summer ozone profile is used, which is scaled so that the total ozone column is the average of the two surface-based Dobson ozone daily measurements at Boulder, Colorado, and Nashville, Tennessee. In this study, the microwave radiometer (MWR) total water vapor column averaged over each 30-minute segment was used to correct the water vapor mixing ratio profile derived from the soundings (Fu et al. 1997).

Aerosol optical depths at wavelengths of 0.413 μm, 0.500 μm, 0.609 μm, 0.664 μm, and 0.860 μm are obtained based on the MFRSR spectral measurements of the solar radiation at the surface, as processed by the narrowband retrieval algorithm of Harrison et al. (1994). The aerosol optical depths used are also 30-minute averages for clear-sky segments. Because the MFRSR measures the optical depths at only five wavelengths, we use the Angstrom relation, $\tau(\lambda) = \alpha\lambda^{-\beta}$, where λ is the wavelength (μm) and α and β are parameters determined by a fit to the MFRSR-derived data, to estimate the aerosol optical depth throughout the shortwave spectrum. For given aerosol optical depths, the diffuse irradiances also depend on aerosol single-scattering albedo and asymmetry factor profiles, which are not available from observation. Here the single-scattering albedo and asymmetry factor from d'Almeida et al. (1991) for the rural aerosol type are adopted in the model simulation where the humidity dependence of aerosol single scattering properties is explicitly considered.

The Fu-Liou delta-four-stream radiation model (Fu and Liou 1993) is employed. Compared with the delta-128-stream model using high spectral resolution for Rayleigh and aerosol scattering, the errors in the calculated fluxes due to the Fu-Liou radiation model are less than about 1 W m^{-2}.

Figure 1 shows the comparison of the downward surface diffuse irradiances between the model calculations and measurements. The 30-minute average results are presented, which contain 119 points covering summer 1996. The model significantly overestimates the surface diffuse irradiances. The mean bias (calculated - observed) is 22.4 W m^{-2} out of the mean observed flux of 97.8 W m^{-2}. The results presented here are consistent with the CAGEX (Charlock and Alberta 1996) Version 1.1.1 analyses and results from Kato et al. (1997) and Kinne et al. (1998). Below, we attempt to find possible explanations for the discrepancy between the model and observations by investigating the potential measurement errors and uncertainties related to the radiative transfer input data.

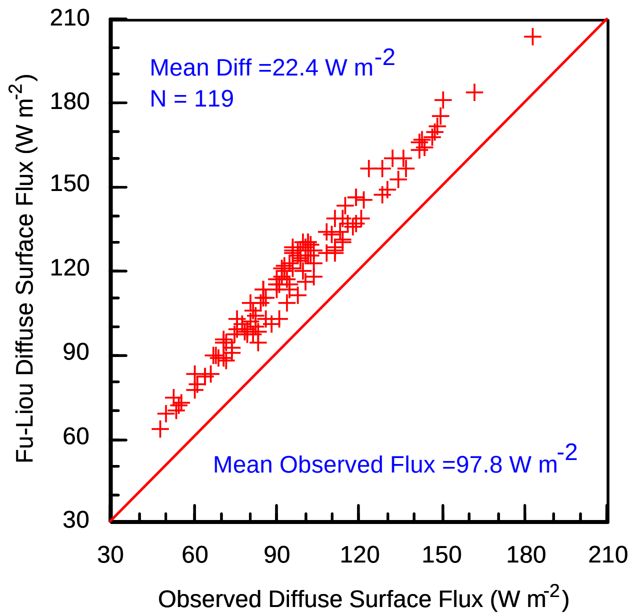

Figure 1. Comparison of 30-minute averaged diffuse surface fluxes between the model and observation for the clear-sky segments in the summer of 1996. In the model simulation, we use the single-scattering albedo and asymmetry factor for the rural aerosol type (d'Almeida et al. 1991). (For a color version of this figure, please see *http://www.arm.gov/docs/documents/technical/conf_9803/fu(3)-98.pdf*.)

Uncertainties in Radiation Measurements and Model Input Data

In addition to the BSRN system, the Solar and Infrared Radiation Observing System (SIROS) consists of another set of radiometers deployed at the ARM SGP central facility for radiation measurements. During the summer of 1996 under clear-sky conditions, we compared the SIROS diffuse field irradiances with those from BSRN, which reveal a mean difference (SIROS-BSRN) of -2.6 W m^{-2} with a standard deviation of 2.7 W m^{-2}. This indicates that the random errors related to shaded pyranometer measurements are small.

The diffuse instruments are calibrated using a cavity radiometer with the direct beam incident at 45° (E. Dutton, personal communication). This is a high-level signal calibration compared to the typical clear-sky diffuse irradiance. To identify potential systematic errors related to the calibration, we examine the nighttime 'observed' diffuse irradiances. For the summer of 1996, the nighttime offset for the BSRN shaded pyranometers ranges from –3 W m^{-2} to -7 W m^{-2} with a mean value of -4.8 W m^{-2}, while for SIROS the nighttime offset is from –4 W m^{-2} to -9 W m^{-2} with a mean value of -6.3 W m^{-2}. By assuming that the daytime instrument offset is the same as that in the nighttime, the shaded pyranometer may underestimate the diffuse fluxes by about 5 W m^{-2} to 6 W m^{-2}. In addition to errors associated with the calibration, the cosine response may cause flux underestimations by about 3 W m^{-2} (Kinne et al. 1998). In total, the systematic errors in measured diffuse irradiances from BSRN can be about -8 W m^{-2}.

Sensitivity studies and data analyses are carried out to examine the effect of uncertainties associated with the radiation model input data. The uncertainty associated with pressure, temperature, water vapor and ozone profiles (Fu et al. 1997) has little impact on the downward diffuse solar irradiances at the surface. For the surface albedo, we used the spectral dependence for pasture. An uncertainty of $\pm$10% in surface albedo introduces differences less than $\pm$1 W m^{-2} in the downward surface diffuse fluxes. Another uncertainty is related to the aerosol optical depth derived from the MFRSR. Halthore et al. (1997) recently compared MFRSR-measured aerosol optical depth with that measured using the Cimel sun photometer at the ARM SGP central facility. They concluded that the aerosol optical depths derived from the two instruments are in agreement to within the accuracy of the measurements. They also showed that the MFRSR aerosol optical depth is systematically smaller than that from the sun photometer by ~0.01 at a wavelength of 0.5 µm. Because the sun photometer uncertainty is smaller than the estimated uncertainty for MFRSR (Halthore et al. 1997), we conclude that the MFRSR may underestimate the aerosol optical depth by ~5.5%. This leads to an underestimation of diffuse irradiances by ~3 W m^{-2} in model simulations. In summary, the systematic errors associated with the shaded pyranometer data and measurements of model inputs may explain ~5 W m^{-2} of the discrepancy between the model results and measurements shown in Figure 1.

In the present study, the major uncertainties are related to the aerosol single-scattering albedo and asymmetry factor, which are determined by the aerosol composition and size distribution. Because we lack composition and size distribution information, we use the single-scattering properties for the rural aerosol type (d'Almeida et al. 1991) in the model simulations. The rural (clean-continental) aerosol consists of water-soluble and dust-like substances, which represent the aerosol type most likely encountered in remote continental areas. The water-soluble component is a mixture of sulfate, nitrate, and organic compounds, while the dust-like substances are mineral dusts representing mid-latitude soil conditions. The water-soluble and dust-like aerosol has similar complex refractive indices at visible wavelengths, which are about ~1.53+0.006i (d'Almeida et al. 1991). Because the ARM SGP central facility is located in a rural area, we assume that the rural aerosol type is most likely present at the measurement site. In the next section, we will use the rural aerosol type to examine the effects of aerosol size distributions on the downward surface diffuse irradiances.

Aerosol Size Distribution Effects on Diffuse Irradiances

d'Almeida et al. (1991) used a lognormal aerosol size distribution in the form

$$\frac{dN}{d\ln r} = \frac{N_o}{(2\pi)^{1/2}\ln\sigma}\exp\left[-\frac{(\ln r - \ln r_m)^2}{2(\ln\sigma)^2}\right],$$

where N is the number of aerosol particles per unit volume with radii less than r, N_o is the total number density, r_m is the geometric mean radius, and σ is the geometric standard deviation. In the single-scattering calculations, d'Almeida et al. used the parameters (r_m, σ) of (0.0285 µm, 2.239 µm) and (0.471 µm, 2.512 µm) for the water-soluble and dust-like aerosol, respectively. The rural aerosol type has an asymmetry factor of 0.6497 µm and single-scattering albedo of 0.9456 µm at the wavelength of 0.55 µm (d'Almeida et al. 1991).

In real atmospheres, the aerosol size distributions are highly variable in space and time. For example, the parameters (r_m, σ) for mineral aerosol can be as small as 0.05 µm, 1.6 µm (d'Almeida et al. 1991). Figure 2 shows the asymmetry factor and single-scattering albedo at a wavelength of 0.55 µm for the rural aerosol as functions of the geometric mean radius with different geometric standard deviations. When r_m is in the Aitken particle mode (0.001 µm < r_m < 0.1 µm), the single-scattering properties are very sensitive to both r_m and σ, which decrease dramatically as r_m or σ decrease. We know that a smaller asymmetry factor and single-scattering albedo will reduce the downward diffuse solar irradiance for a given aerosol optical depth. Therefore, to bring the model results into agreement with observations, we suggest that the aerosol geometric mean radius at the ARM SGP central facility is in the Aitken particle mode. We further suggest that the geometric standard deviation should be smaller than 2 if 0.01 µm < r_m < 0.1 µm.

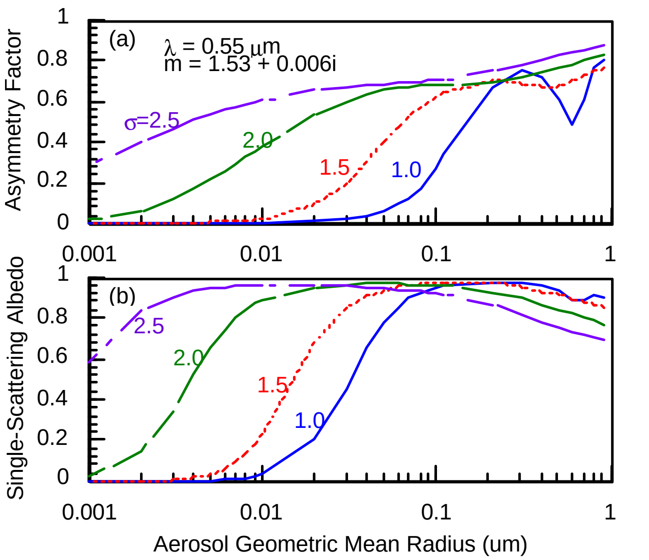

Figure 2. Asymmetry factor (a) and single-scattering albedo (b) as functions of the geometric mean radius and standard deviation for the rural aerosol at the wavelength of 0.55 µm from Mie calculations. (For a color version of this figure, please see *http://www.arm.gov/docs/documents/technical/conf_9803/fu(3)-98.pdf*.)

In order to test the above hypothesis and indicate how the aerosol size distribution might affect the diffuse field irradiances, a simple exercise is performed using the lognomal aerosol size distribution with a constant standard deviation of 1.5. For each case in Figure 1, we reduce the aerosol asymmetry factor and single-scattering albedo by reducing its geometric mean radius until the differences between the simulated diffuse irradiances and the measurements are less than 5 W m^{-2}. The 5 W m^{-2} difference is chosen to account for the systematic measurement errors. Figure 3a shows the comparison of downward diffuse irradiances between the model and measurements after adjusting r_m, which indicates that for each case the model results can be brought into agreement with observations through adjusting the aerosol size distribution. Figure 3b shows the adjusted single-scattering albedo as a function of the adjusted asymmetry factor. The adjusted single-scattering albedo ranges from 0.67 µm to 0.96 µm with a mean value of 0.90 µm, while the adjusted asymmetry factor is from 0.1 µm to 0.48 µm with a mean value of 0.30 µm. This corresponds to a geometric mean radius from ~0.02 µm to ~0.065 µm with a mean value of ~0.04 µm. Assuming that the aerosols are confined in the lower atmosphere from the surface to 3 km, the number concentration derived is ~4.5 x 10^4 cm^{-3} using a r_m of 0.04 µm for an aerosol optical depth of ~0.15. It should be noted that in this exercise we use a constant standard deviation of 1.5, which can be a variable in real atmospheres. Also, if we use a larger σ, the required r_m would be smaller.

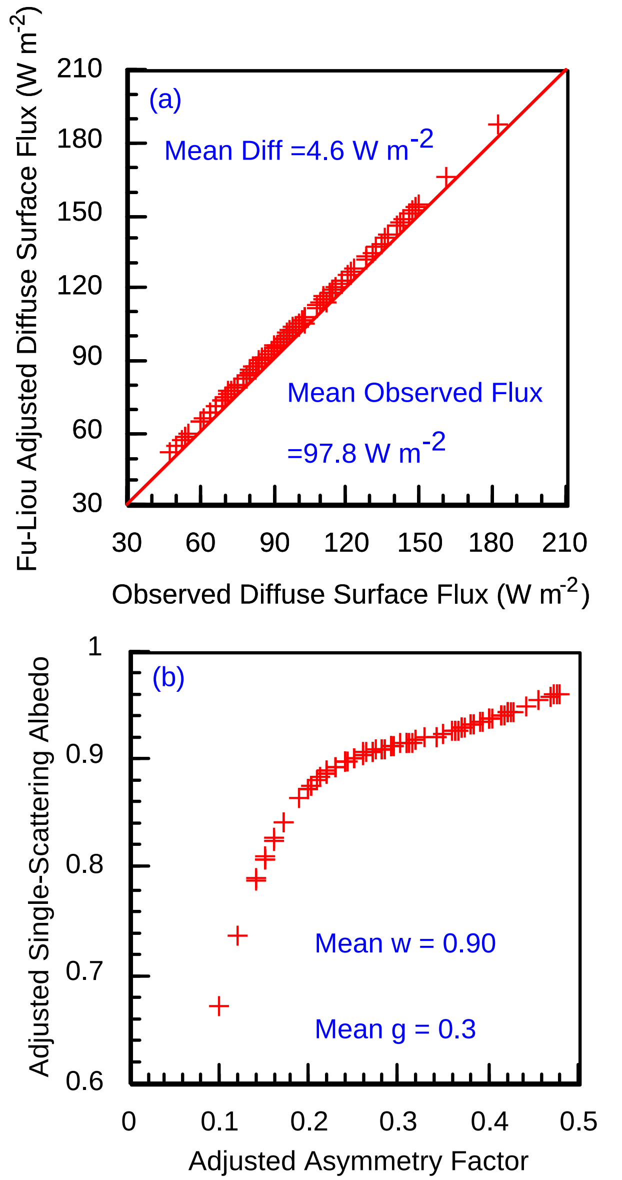

Figure 3. (a) Comparison of diffuse surface fluxes between the adjusted model results and observation. (b) Adjusted single-scattering albedo versus adjusted asymmetry factor. In the model simulation, we adjust the single-scattering albedo and asymmetry factor by reducing aerosol geometric mean radius. (For a color version of this figure, please see *http://www.arm.gov/docs/documents/technical/conf_9803/fu(3)-98.pdf*.)

The aerosol observing system located at the ARM SGP central facility provides in situ aerosol measurements at the surface (M. D. Cheng, personal communication). This system measures the surface aerosol single-scattering albedo at the wavelength of 0.55 μm by using two nephelometers and one light absorption photometer. The measured single-scattering albedo in the summer of 1996 ranges from 0.65 μm to 0.98 μm with a mean value of 0.91 μm, which is consistent with our model-derived single-scattering albedo.

The hypothesis regarding the aerosol size distributions is also consistent with our knowledge of aerosol processes. The relative humidity in the clear-sky conditions we analyzed is less than 70%. Twomey (1977) suggested that in the dry state most atmospheric aerosol particles are smaller than 0.1 μm and are produced initially from trace gases. The ultrafine particles (<0.01 μm) are quickly converted into larger aerosols by coagulation due to the Brownian diffusion. Because the mobility of aerosols decreases rapidly as their sizes increase, coagulation is essentially confined to aerosol less than ~0.1 μm (Wallace and Hobbs 1977). Generally speaking, the small end of the aerosol size distribution changes quickly due to the diffuse effects and the large end is modified by the effects of inertia. However, a greater stability is found in the radius range about 0.03 μm to 0.1 μm where both diffusion and sedimentation are small (Twomey 1977). Aerosol between 0.01 μm and 0.1 μm are collected most efficiently by the nucleation and diffusiophoresis during cloud processing (Wallace and Hobbs 1977; Twomey 1977).

Discussions and Conclusions

Due to the lack of measurements concerning the aerosol composition and size distributions, large uncertainties exist in the comparison of model and observations for the clear-sky radiative energy budget. Using the First International Satellite Cloud Climatology Program (ISCCP) Regional Experiment (FIRE) 1991 field experiment data, Kinne et al. (1998) analyzed clear-sky solar transmission by assuming a sulfuric acid solution aerosol. They used a log-normal aerosol size distribution with a r_m of 0.10 μm and a σ of 2. Charlock and Alberta (1996) used the d'Almeida et al. (1991) rural aerosol type in the CAGEX Version 1.1.1 analyses. In both studies, the single-scattering albedo and asymmetry factor are prescribed.

In the study for the ARM Enhanced Shortwave Experiment (ARESE) period, Kato et al. (1997) retrieved the aerosol size distribution using measured aerosol optical depths at different wavelengths. For the mineral aerosol type, they obtained an asymmetry factor of ~0.69 and a single-scattering albedo of ~0.91. Figure 4 shows the Angstrom exponent β as a function of the aerosol radius for different aerosol types based on Mie simulations. The β is sensitive to both aerosol composition and size. The most striking feature in Figure 4 is that for weak absorbing aerosol such as water-soluble type, specifying β does not uniquely determine the aerosol size. The Angstrom exponent is also related to aerosol refractive indices and their wavelength dependence. Unfortunately, reliable laboratory measurement of refractive indices are lacking for most of the aerosol chemical species.

In this study, a hypothesis regarding the effects of the aerosol size distribution is examined in an attempt to bring the model results into agreement with observations of the diffuse irradiances. By analyzing the data from the ARM SGP central facility under clear-sky conditions, it was suggested that the aerosol may be largely in the Aitken particle mode (0.01 μ - 0.1 μm). It should be noted that the uncertainty related to the daytime radiometer offset and the effect of aerosol composition might still be highly significant. The important issue here, however, is that the discrepancy between the model and observations has highlighted the need for a closure experiment, which requires accurate radiation measurement and an observing strategy for the information regarding the aerosol composition and size distribution profiles.

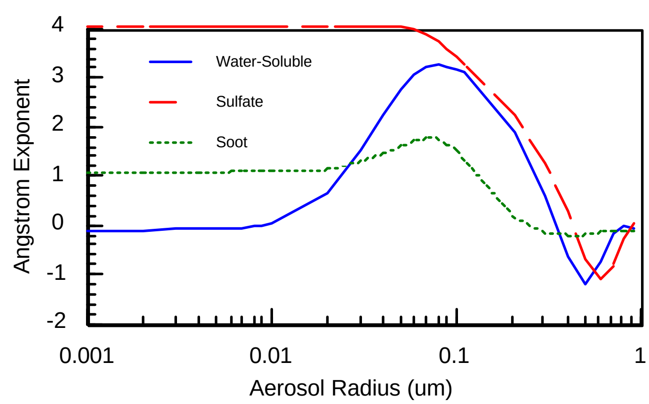

Figure 4. Angstrom exponent as a function of the aerosol radius for water-soluble, sulfate, and soot aerosol. (For a color version of this figure, please see *http://www.arm.gov/docs/documents/technical/conf_9803/fu(3)-98.pdf*.)

Acknowledgments

We are indebted to E. Dutton for information on the BSRN instrument and M. D. Cheng for assisting on the ARM data. We wish to thank T. Charlock, P. Chylek, N. Fukuta, Z. Li, and W. Wiscombe for useful discussions. The research work contained herein has been supported by DOE Grant DE-FG02-97ER62363, and in part by NSERC Operating Grant, and NSERC Collaborative Grant.

References

Charlock, T. P., and T. L. Alberta, 1996: The CERES/ARM/GEWEX experiment (CAGEX) for the retrieval of radiative fluxes with satellite data. *Bull. Amer. Meteor. Soc*., **77**, 2673-2683.

d'Almeida, G., P. Koepke, and E. P. Shettle, 1991: *Atmospheric Aerosols-Global Climatology and Radiative Characteristics.* A. Deepak, 561 pp.

Fu, Q., and K. N. Liou, 1993: Parameterization of the radiative properties of cirrus clouds. *J. Atmos. Sci*., **50**, 2008-2025.

Fu, Q., G. Lesins, J. Higgins, T. P. Charlock, P. Chylek, and J. Michalsky, 1997: Water vapor continuum absorption of solar radiation tested using ARM data. *Geophys. Res. Lett*., **25**, 1169-1172.

Halthore, R., et al., 1997: Comparison of model estimated and measured direct-normal solar irradiance. *J. Geophys. Res*., in press.

Harrison, L., J. Michalsky, and J. Berndt, 1994: Automated multifilter rotating shadow-band radiometer: An instrument for optical depth and radiation measurements. *Appl. Opt*., **33**, 5118-5132.

Kato, S., et al., 1997: Uncertainties in modeled and measured clear-sky surface shortwave irradiances. *J. Geophys. Res*., **102**, 25,881-25,898.

Kinne, S., R. Bergstrom, O. B. Toon, E. Dutton, and M. Shiobara, 1998: Clear sky atmospheric solar transmission: An analysis based on FIRE 1991 field experiment data. *J. Geophys. Res*., in press.

Stokes, G. M., and S. E. Schwartz, 1994: The Atmospheric Radiation Measurement (ARM) Program: Programmatic background and design of the cloud and radiation test bed. *Bull. Am. Met. Soc*., **75**, 1201-1221.

Twomey, S., 1977: *Atmospheric Aerosols*. Elservier, 302 pp.

Wallace, J. M., and P. V. Hobbs, 1977: *Atmospheric Science an Introductory Survey*. Academic Press, 467 pp.